

Structural and Optical Properties of Pure and Transition Metal Ion Doped SnO₂ Quantum Dots

S.Chitra^{1*}, D. Easwaramoorthy², S. Nalini Jayanthi³, S.Shanthi⁴

¹Department of Chemistry, Jeppiaar Engineering College, Chennai, India

²Department of Chemistry, B.S. Abdur Rahman University, Chennai, India

³Department of Physics, KCG College of Technology, Chennai, India

⁴Department of Chemistry, Anand Institute of Higher Technology, Chennai, India

*Corres.author: chitra_sethumurugan@yahoo.com, *Phone :9003025980

Abstract: Pure and transition metal ion (Zn²⁺, Cd²⁺ and Ni²⁺) doped SnO₂ quantum dots was synthesized by simple microwave irradiated solvothermal (MIS) method. The morphology of pure and doped SnO₂ quantum dots was confirmed by SEM images. The nanocrystal structure and crystallite size analysis was done by PXRD. The addition of dopants (Zn²⁺, Cd²⁺ and Ni²⁺) in the host SnO₂ lattices increases the nanocrystalline size. The average crystallite sizes and lattice strain of all the synthesized pure and doped SnO₂ nanocrystals was calculated by Debye-Scherrer equation and Williamson-Hall plot. Variation in the bandgap of pure and doped SnO₂ was explained by UV-Vis and PL spectral analysis. The photoconducting properties, rise and decay of photocurrent for pure and doped SnO₂ was also analysed.

Keywords: Solar cell, SEM,TEM, W-H PLOT, Crystallite size , Band gap, Photoconductivity.

1. Introduction:

Nanoparticles or quantum dots have received considerable attention due to the quantum phenomena resulting from the change in band gap with higher oscillator strength [1]. SnO₂ has gained prominence in technological field due to its interesting electrical and optical properties arising out of large surface-to-volume ratio, quantum confinement effect etc and has been applied in many applications such as transparent conducting coating of glass, gas sensors, solar cell and heat mirror [2-4]. Nanocrystalline SnO₂ semiconductor with bandgap energy 3.6eV has the tetragonal rutile structure in which the oxygen vacancies act as electron acceptor [5]. The MIS method was used to synthesize highly stable undoped and doped SnO₂ nanoparticles of crystallite sizes below 7 nm. The synthesis procedure is highly reproducible, low-cost and easily scaled-up. In this present investigation pure and 5 mole % of Zn²⁺, Cd²⁺ and Ni²⁺ doped SnO₂ quantum dots were synthesized. They can be used as the photoanodes in Dye Sensitized Solar Cells (DSSCs) which showed an improvement in energy conversion efficiency. The substitution of dopants in SnO₂ shifts the excitonic peaks to higher wavelength side which helps to tune the optical band gap energy.

2. Materials and Methods:

Pure SnO₂ nanocrystals was synthesized by dissolving 0.6 mole of CO(NH₂)₂ in 50 ml of ethylene glycol under vigorous stirring condition for 1 hour at room temperature. Subsequently 0.2 mole SnCl₄ solution was added in 50 ml ethylene glycol and then added slowly into the above solution. This solution was stirred for another 1 hour at 60 °C temperature. The resulting dissolved mixture is clear and deep blue in colour and it is called as stock solution.

The stock solution was kept in a domestic microwave oven and irradiated with 30% of maximum power until the solvent gets evaporated completely. The resultant product obtained in the form of colloidal precipitate was cooled to room temperature and centrifuged several times with doubly distilled water and the unreacted reactants and organic impurities present in the colloidal precipitate was removed with acetone. Then the centrifuged final product was dried in an oven at 60 °C for 10 hour and collected as the yield. 5 wt. % ZnCl₂, CdCl₂ and NiCl₂ was added separately to the stock solution in the case of preparing SnO₂:Zn²⁺, SnO₂:Cd²⁺ and SnO₂:Ni²⁺ nanocrystals respectively using the procedure as similar to the above. All the Chemicals were of analytical reagent grade purity (99.9%) and used as purchased from sigma-Aldrich and Merck India Ltd without further purification.

3. Results and Discussion

3.1 Structural Properties

3.1.1 XRD Analysis

Powder X-ray diffraction spectra for pure and doped SnO₂ nanocrystals annealed at 600°C were recorded in the room temperature and shown in fig 1. Diffraction pattern will give the information about crystalline structure and crystallite size of nanoparticle. The diffraction peaks in the XRD patterns are indexed with the standard JCPDS file no 41-1445. All the prominent peaks in the pattern confirmed the formation of SnO₂ tetragonal rutile type structure with the space group p4₂/mm of polycrystalline SnO₂ and have been indexed on the basis of JCPDS file. No additional phase such as ZnO, CdO and NiO is observed, indicating the successful doping of Zn²⁺/ Cd²⁺/Ni²⁺ ions into the host SnO₂ lattices. The broadening of the diffraction peaks indicates the nanosize of the synthesized particles. It has observed that there is slight change in the peak position of XRD spectra with respect to addition of dopants. However the tetragonal rutile-type structure remains the same for both the pure and doped SnO₂ nanocrystals. The average crystallite size of pure and doped SnO₂ nanocrystals was calculated by measuring full-width half-maximum (FWHM) of the most intense diffraction peaks (110), (101), (200) and (211) using Debye-Scherrer equation and W-H plot. Calculated lattice parameters for pure and different dopant added SnO₂ nanocrystals are given in table 1 & Calculated crystallite size and lattice strain for pure and different dopant added SnO₂ nanocrystals from Scherrer formula and W-H plots are given in table 2.

Table 1: Calculated lattice parameters for pure and different dopant added SnO₂ nanocrystals (*JCPDS file no 41-1445)

Quantum dots	Lattice parameter (Å)		Unit cell Volume Å ³
	a=b	c	
*SnO ₂ (rutile-type)	4.7382	3.1871	71.552
Pure SnO ₂	4.7223	3.1398	70.018
SnO ₂ :Zn ²⁺	4.7337	3.1027	69.525
SnO ₂ :Cd ²⁺	4.7617	3.1987	72.526
SnO ₂ :Ni ²⁺	4.7062	3.1178	69.054

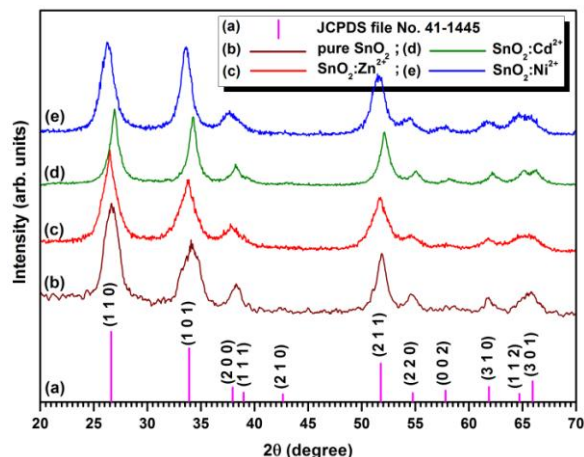


Figure 1 Powder XRD patterns of pure and different dopant added SnO₂ nanocrystals annealed at 600 °C temperatures

Table 2: Calculated crystallite size and lattice strain for pure and different dopant added SnO₂ nanocrystals from Scherrer formula and W-H plots

Quantum dots	Crystallite size (nm)		Lattice strain from W-H plot x 10 ⁻³
	From Scherrer (±0.23)	From W-H plots (±0.14)	
Pure SnO ₂	4.36	4.40	0.525
SnO ₂ :Zn ²⁺	3.82	3.97	1.083
SnO ₂ :Cd ²⁺	5.98	6.60	1.693
SnO ₂ :Ni ²⁺	3.52	3.35	-1.586

3.1.2 SEM and TEM Analysis

SEM and TEM images were recorded for pure and doped SnO₂ nanocrystals and the recorded images were shown in fig 2(a) - 2(d) & fig 3(a) - 3(d). SEM micrographs show the presence of large spherical aggregates of smaller individual nanoparticles.

The morphologies of all the samples in TEM micrographs are found to be nearly spherical in nature with the diameters ranging from 5 to 8 nm. It clearly indicates that the average particle size varies with an addition of dopant in the host SnO₂ nanocrystals. From the TEM micrographs it was concluded that the addition of Zn²⁺ and Ni²⁺ restricts the growth of crystallites in the host SnO₂ nanocrystals and the addition of Cd²⁺ enhances the growth of crystallites in the host SnO₂ nanocrystals. Ni²⁺ and Cd²⁺ doped SnO₂ nanocrystals possess highly dispersed spherical particles. In the case of Zn²⁺ doped SnO₂ nanocrystals highly aggregated particles were obtained. It clearly shows that the average particle size of all the synthesized samples are in the nanoscale. It also inline with the result of SEM analysis. The mean particle size determined by TEM is in good agreement with the average particle size calculated by Scherrer's formula and W-H plots from the XRD patterns.

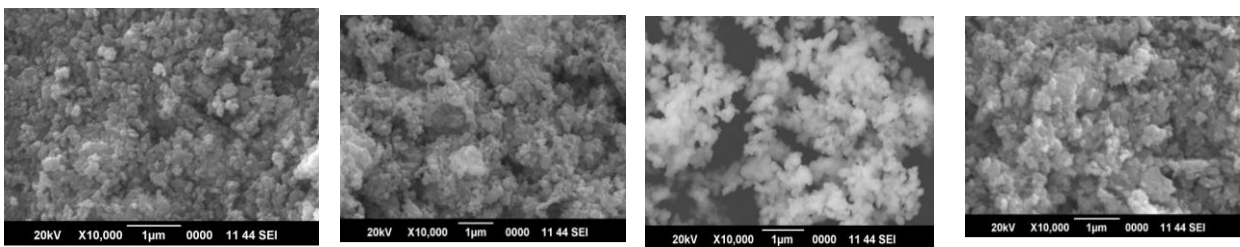


Fig.2(a): SEM image pure SnO₂ Fig.2(b): Zn²⁺doped SnO₂ Fig.2(c): Cd²⁺doped SnO₂ Fig.2(d): Ni²⁺doped SnO₂

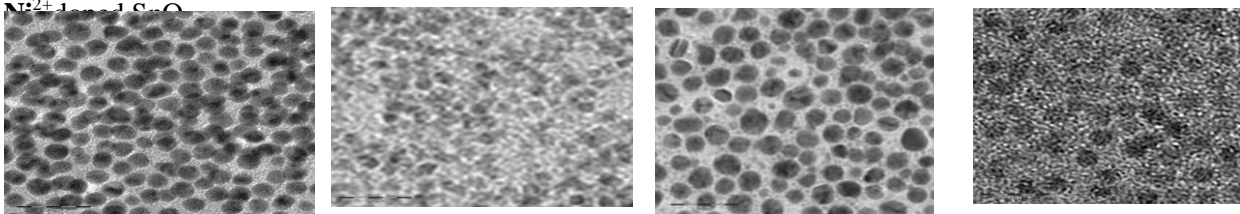


Fig.3(a): TEM image pure SnO₂ Fig.3(b): Zn²⁺doped SnO₂ Fig.3(c): Cd²⁺doped SnO₂ Fig.3(d): Ni²⁺doped SnO₂

Comparison of Calculated crystallite size for pure and different dopant added SnO₂ nanocrystals from Scherrer formula , W-H plots and TEM images are given in table 3.

Table 3 : Comparison of Calculated crystallite size for pure and different dopant added SnO₂ nanocrystals from Scherrer formula , W-H plots and TEM images

Quantum dots	Crystallite size (nm)		From TEM images Crystallite size (nm)
	From Scherrer (±0.23)	From W-H plots (±0.14)	
Pure SnO ₂	4.36	4.40	6.34 (± 0.11)
SnO ₂ :Zn ²⁺	3.82	3.97	5.83 (± 0.09)
SnO ₂ :Cd ²⁺	5.98	6.60	7.62 (± 0.15)
SnO ₂ :Ni ²⁺	3.52	3.35	5.23 (± 0.14)

3.2 Optical Properties

3.2.1 UV-Vis Spectral Measurement

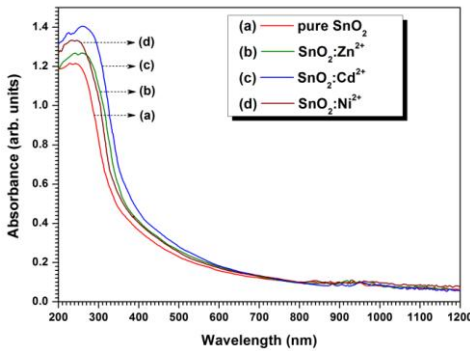


Fig 4 a): UV-Vis. absorbance spectra of pure and doped SnO₂ nanocrystals

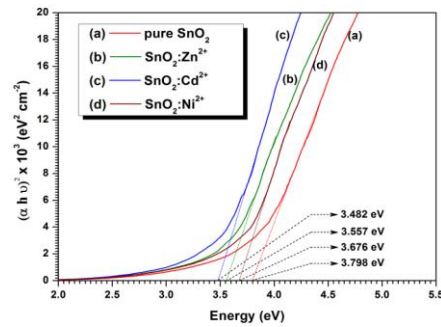


Fig 4(b):Plots of $(\alpha h\nu)^2$ versus $h\nu$ for pure and doped SnO₂ nanocrystals

UV-Vis absorption spectra were recorded for pure and doped (Zn²⁺, Cd²⁺ and Ni²⁺) SnO₂ nanocrystals in the wavelength range of 200–1200 nm. The recorded spectra are shown in Fig 4(a) & 4(b). The absorption edge of the pure and doped SnO₂ nanoparticles varies with respect to different dopants. The absorption edge and optical bandgap of the prepared samples were calculated by Tauc's relation [6]. The optical band gap for the absorption peak can be obtained by extrapolating the linear portion of the plot to energy ($h\nu$) axis. The measured bandgap values are given in Table 4. The measured optical bandgap for pure SnO₂ is 3.798 eV (326 nm) which are slightly higher than that of bulk SnO₂ i.e., 3.6 eV (344 nm). This blue shift in optical bandgap for pure SnO₂ can be attributed to the quantum confinement effect of the nanoparticles [7].

Table 4 : Calculated optical bandgap energies and visible emission band energy for pure and doped SnO₂ nanocrystals from UV-Vis. and PL spectra (* optical bandgap of bulk SnO₂ material reported by Lee et al. (2004))

Sl. No	Quantum dots	Optical bandgap energy		Visible emission band energy from PL (± 0.016 eV)
		From UV-Vis. (± 0.019 eV)	From PL (± 0.021 eV)	
1	*Bulk SnO ₂	3.6	-	-
2	Pure SnO ₂	3.798	3.765	2.407
3	SnO ₂ :Zn ²⁺	3.557	3.519	2.235
4	SnO ₂ :Cd ²⁺	3.482	3.457	2.227
5	SnO ₂ :Ni ²⁺	3.676	3.639	2.278

The substitution of Zn²⁺, Cd²⁺ and Ni²⁺ in Sn⁴⁺ sites, the excitonic absorption peak leads to shift in higher wavelength side (red shift). The shifting of band gap towards higher wavelength side (red shift) suggests the addition of dopants in the host SnO₂ lattices helps to tune the optical bandgap energy. It may be suggested that the variation in energy bandgap will be suitable for window material for fabrication of solar cells.

3.2.2 Photoluminescence Analysis

The PL emission spectra of the pure SnO₂ and 5wt% Zn²⁺, Cd²⁺ and Ni²⁺ doped SnO₂ nanocrystals excited at a wavelength of 250nm at room temperature are shown in fig 5. A weak UV emission band around 329 nm and a strong bluish green broad emission around 515nm are present in pure SnO₂ nanocrystals. The UV emission is due to near band edge (NBE) emission. The bluish green emission is due to defect emission in the visible region. This is due to the crystal defects or defect levels within the bandgap of SnO₂ associated with the oxygen vacancies or Sn interstitials, dangling bond and structural defects that have formed during growth [8-10]. Similar behavior was obtained for the doped SnO₂ nanocrystals. The position of NBE band for doped SnO₂ nanocrystals is shifted to higher wavelength side and emits UV radiation. Also the position of strong broad emission band is slightly red shifted and emits green radiation. With the addition of dopant into the parent

SnO₂ lattices, the UV emission and the green emission intensities increases. This is due to the defect and particle size affected by doping ions in the host SnO₂ nanocrystals which can create oxygen vacancies in the crystal lattice and the donor level is enhanced. The increase in donor level increased the PL intensity in doped SnO₂ nanocrystals [11]. The presence of small amount of dopants (5 wt. % of Zn²⁺, Cd²⁺ and Ni²⁺) greatly affects the PL intensity of the host SnO₂ nano crystals. This significant red shift provides clear evidence for the formation of the doped nanocrystals (SnO₂:Zn²⁺, SnO₂:Cd²⁺ and SnO₂:Ni²⁺) rather than forming separate ZnO, CdO, NiO or a mixed phase structured nanocrystals.

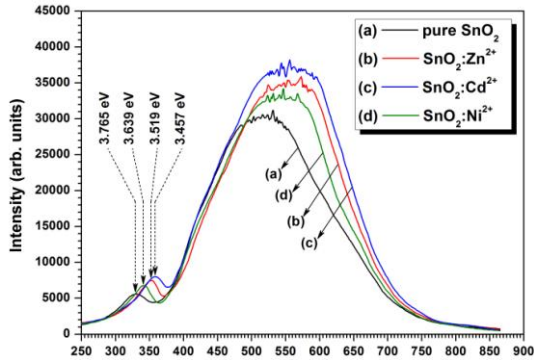


Fig 5: Photoluminescence emission spectra of pure and doped SnO₂ nanocrystals

The doped nanocrystals (SnO₂:Zn²⁺, SnO₂:Cd²⁺ and SnO₂:Ni²⁺) leads to strong enhancement in hotoluminescence yield compared to pure SnO₂ and consequently they can be used as the new useful materials for photonic applications. [11]

3.3 Photoconductivity properties

The variation of field dependence dark current (I_d) and photocurrent (I_p) with applied voltage (V) for pure and doped (Zn²⁺, Cd²⁺ and Ni²⁺) SnO₂ are shown in Fig 6(a) & 6(b). It is observed that both dark and photo currents of pure and doped SnO₂ nanocrystals increase linearly with the applied voltage. The photocurrent of both pure and doped SnO₂ nanocrystals is more than the dark current, which is termed as positive photoconductivity. All the synthesized pure and doped SnO₂ nanocrystals considered in the present study are found to exhibit positive photoconductivity. This is due to the absorption of photons by mobile charge carriers present in the samples (pure and doped) [12]. In the present investigation it was observed that photocurrent is more for doped SnO₂ nanocrystals than that of pure SnO₂ nanocrystal. The defect states introduced by incorporation of Zn²⁺, Cd²⁺ and Ni²⁺ inside the SnO₂ lattices increases the dark and photocurrent by nearly two orders.

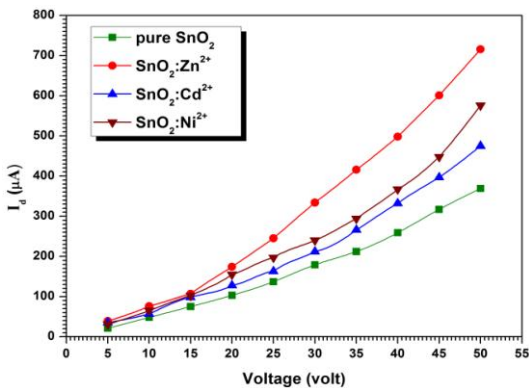


Fig 6(a)

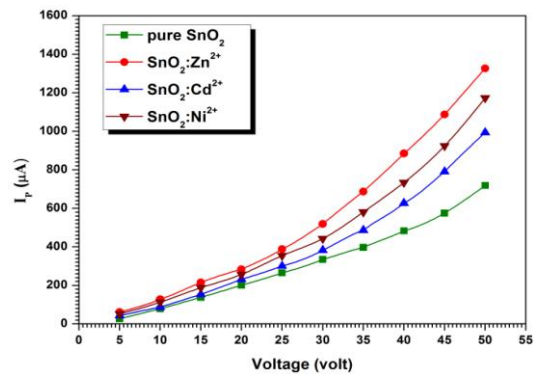


Fig 6(b)

Fig 6(a) : Variation of dark current with applied voltage for pure and doped SnO₂ nanocrystals

Fig 6(b) : Variation of photo current with applied voltage for pure and doped SnO₂ nanocrystal

The time-resolved rise and decay of photocurrent spectras were recorded for pure and doped SnO₂ nanocrystals at low intensity(75watts) and high intensity(150 watts). The time-resolved rise and decay of photocurrent spectra for undoped as well as different doped (Zn²⁺ Cd²⁺ and Ni²⁺) SnO₂ nanocrystals are shown in Fig 7(a & b).

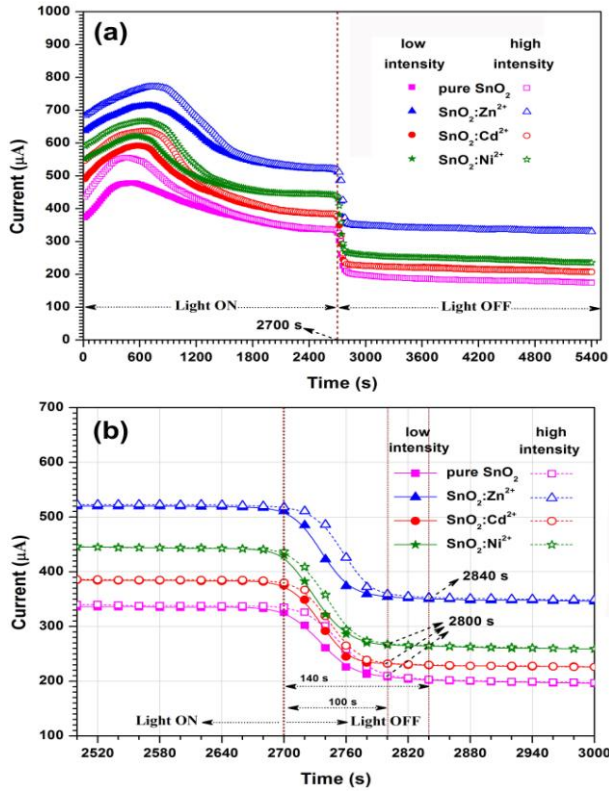


Fig 7(a) &(b)

Fig 7 : (a) Variation of time resolved rise and decay of photocurrent with different light intensity spectra of pure and doped SnO₂ nanocrystals (b) the same spectra in expanded scale

All the nanocrystals both pure and doped SnO₂ under steady state illumination (in both the low and high intensity condition) exhibit anomalous behavior. Such anomalous behavior was reported in ZnO nanowire, Co-doped ZnO nanobelts etc [13-15]. As the illumination intensity increased to high value (150 watt), the photocurrent initially increases in all the samples which are higher than that of low intensity value. This may be due to fast process of generation of electron-hole pairs as a result of absorption of photons which increases the photocurrent. The time taken for attaining maximum value of photocurrent is nearly 100 to 260 seconds higher than that of low intensity illumination. The doped SnO₂ samples took more time to reach maximum photocurrent value than the pure SnO₂ sample (Fig 8) due to defect states introduced by the incorporation of Zn²⁺, Cd²⁺ and Ni²⁺ into the host SnO₂ lattices. The Photocurrent decreases exponentially within few seconds when illumination is switched off and attains a constant value for a long time. The doped samples will take more than 40s than that of pure SnO₂ sample to attain constant value. The decrease in the photocurrent is due to the electron-hole pairs recombine with each other and is captured by re-adsorbed oxygen molecules [16-17].

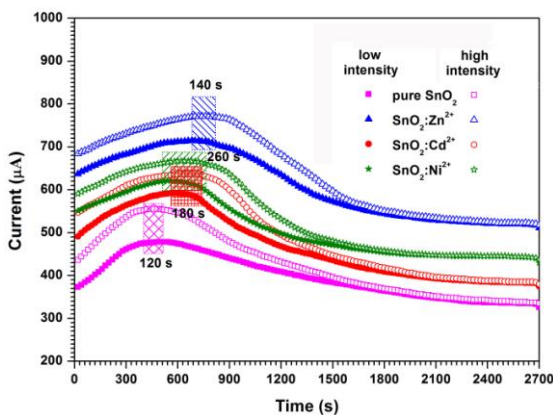


Fig 8: Variation of time resolved rise and decay of photocurrent with different light intensity spectra of pure and doped SnO₂ nanocrystals when light ON mode.

Conclusion

Pure and Zn²⁺, Cd²⁺ and Ni²⁺ SnO₂ quantum dots was successfully synthesized by simple microwave solvothermal method. The formation of oxygen defects at grain boundary region is very low and hence even at doped condition rutile phase of SnO₂ is formed. Our synthesis technique yielded highly pure and lesser crystallite size of SnO₂ nanocrystals. The TEM images concludes that this preparation method was successful to obtain pure and doped SnO₂ nanoparticles with smaller crystallite size. The shifting of bandgap in UV towards higher wavelength side (red shift) suggests the addition of dopants in the host SnO₂ lattices helps to tune the optical bandgap energy. The addition of dopant in the SnO₂ lattices creates oxygen vacancies in the crystal lattice and the donor level is enhanced. The increase in donor level increases the PL intensity in doped SnO₂ nanocrystals. It may be suggested that the variation in energy bandgap for pure and doped SnO₂ quantum dots will be suitable for using as a window material for fabrication of solar cells. The prepared nanocrystals can be able to harvest visible component of solar radiation and therefore these nanocrystals could be used as the photocatalysts under visible light.

References

1. Shan B, Lakatos G W, Peng S, Cho K, Appl. Phys. Lett., 2005, 87, 173109.
2. Dieguez A, Romano-Rodriguez A, Morante J.R, Weimar U, Schweizer-Berberich M, Gopel W, Morphological analysis of nanocrystalline SnO₂ for gas sensor applications, sens. Actuators B: Chem. 1996, 31, 1-8.
3. Kudo N, Shimazaki Y, Ohkita H, Ohoka M, Ito S, Organic-inorganic hybrid solar cells based on conducting polymer and SnO₂ nanoparticles chemically modified with a fullerene derivative, Solar Energy Mater. Solar cells 2007, 91, 1243-1247
4. Choudhury C, Sehgal H.K, Chemical vapour deposited SnO₂: Sb heat mirror coatings for cylindrical solar collectors, Energy Convers. Manage. 1989, 29, 265-272.
5. Chen Z, Lai J KL, Shek C.-H, Chen H, J. Mater. Res., 2003, 18, 1289.
6. Tauc J, Grigorovici R, Vancu A, Optical properties and electronic structure of amorphous Germanium, Phys. Status Solidi b, 1966, 15, 627-637.
7. Takagahara T and Takeda K, Physical Review B, 1992, 46, 15578-15581.
8. Hu J, Bando Y, Liu Q, Golberg D, Adv. Funct. Mater. 2003, 13, 493.
9. Cheng B., Russell J M, Shi W, Zhang L, Samulski E T, J. Am. Chem. Soc. 2004, 126, 5972.
10. Chang S.-S and Park D.K, Mater. Sci. Eng. B, 2002, 95, 55.
11. Kim T W, Lee D U, Yoon Y S, Journal of Applied Physics, 2000, 88, 3759.
12. Joshi V N, Photoconductivity, Marcel Dekker, New York, 1990
13. Ahn S E, Ji H J, Kim K, Kim G T, Bae C H, Park S M, Kim Y K, Ha J S, Appl.Phys.Lett. 2007, 90, 153106.
14. Peng L, Zhai J.-L, Wang D.-J, Wang P, Zhang Y, Pang S, Xie T.-F, Chem. Phys. Lett.2008, 456, 231.
15. Bera A and Basak D, Appl. Phys. Lett. 2009, 94, 163119.
16. Liao Z.-M, Xu J, Zhang J.-M, Yu D.-P, Appl. Phys. Lett. 2008, 93,023111.
17. Zheng X G, Sh Q. Li, Hu W, Chen D, Zhang N, Shi M J, Wang J J., Zhang Ch L, J.Lumin2007, 122,198.
18. Lee E J H, Ribeiro C, Giraldi T R, Longo E and Leite E R, Photoluminescence in quantum-confined SnO₂ nanocrystals: Evidence of free exciton decay, Appl. Phys. Let. 2004, 84, 1745 - 1747.
